Hindawi
Journal of Electrical and Computer Engineering
Volume 2023, Article ID 2590362, 13 pages
https://doi.org/10.1155/2023/2590362

Research Article

Optimal Operation of Energy Hub Systems under Resiliency Response Options

Ali Khodadadi, Taher Abedinzadeh, Hasan Alipour, and Jaber Pouladi

Department of Electrical Engineering, Shabestar Branch, Islamic Azad University, Shabestar, Iran

Correspondence should be addressed to Taher Abedinzadeh; taherabedinzade@yahoo.com

Received 29 October 2022; Revised 14 December 2022; Accepted 19 December 2022; Published 10 January 2023

Academic Editor: Yang Li

The economic and resilient operation of power systems has always been one of the main priorities of energy systems. In spite of improvements in various fields of energy systems, especially power systems, the issue of resilience has become more important. For this purpose, this paper proposes a multiobjective optimization model to improve the economic performance of energy hub systems and improve the resilience of electrical consumers. Also, consumer welfare, which is a function of the energy not supplied index, is maximized over a 24-hour period by considering extreme weather conditions. The ε-constraint method is applied to solve the proposed model by transforming the multiobjective optimization problem into several single-objective optimization problems. The max-min fuzzy method is also used to select the optimal solution among the Pareto solutions. A sample hub system is made up of electrical, thermal, and gas loads, electrical and thermal energy sources, and storage systems employed as a test system. A group of actions is applied to improve the resilience of the system, which may be affected by outages caused by storms under the resilience response program (RRP). The results proved the efficiency of the proposed RRP in improving economics and resilience.

1. Introduction

By integrating different energy systems, including various sources with high operating efficiencies, under the concept of the energy hub, highly flexible energy systems with favorable performance can be produced. Energy hub systems can optimally supply energy demand by utilizing multiple energy sources and energy transformations, which will increase their flexibility, while other expected targets, such as the resilience of system indices, are met as much as possible.

In recent years, energy hub systems have been studied from a variety of aspects, including economic performance, uncertainty modeling, sustainability, reliability, and resiliency [1–3]. The optimal performance of interconnected hub systems has been studied in [4], considering the reliability of the system, in which the minimal cut-maximal flow method is used to examine the energy flux in the energy hub system. In this system, the energy not supplied (ENS) index has been used to assess the resiliency of the supply. The optimal performance of medium-sized and large-sized energy hub systems has been investigated with a linear-numerical programming approach in [5], where the total cost of the energy hub system, including investment and operation costs, has been minimized and the ENS index has been computed to evaluate the system performance. Optimum dispatching of the energy hub system under a reliability-based method has been studied in [6], in which indices such as the ENS and loss of load expectation have been used to evaluate the system's reliability. The optimal performance of the energy hub system has been studied with mathematical programming by considering the system reliability and uncertainties associated with renewable resources, load, and price [7, 8].

Focusing on energy diversity, the optimal performance of multicarrier systems has been examined by considering the potential probability of resource capacity [9]. To provide effective resiliency for different loads, the optimal design of energy hub systems has been studied by using the resiliency indices under a linear model [10]. In [11], an optimization model has been presented for optimal planning of energy hub systems, consisting of different energy networks, in which the cost of investment in production units under various constraints, such as environmental and energy efficiency constraints, has been minimized. The optimal performance of energy hub buildings has been studied by taking into account the robustness of the energy demand [12] in which, contrary to other researchers, the dynamic behavior of thermal loads has been considered in assessing system security under the Markov chain concept. A similar work is referred to in [13] that is based on information-gap decision theory to ensure robust operation of the hub energy system by considering uncertainties such as demand and outages in the electrical section of the hub that may be caused by weather conditions. To investigate the optimal performance of active distribution networks, an optimization model has been presented in [14] under the concept of a renewable-energy hub, in which the availability of distributed generation resources, as well as electric vehicles capable of being connected to the network under probability methods, has been studied. To determine the optimal size of combined heat and power (CHP) systems in integrated gas-electric networks, an optimization model has been presented in [15], in which the system cost, power losses, and reliability are investigated. A two-level optimization model for optimal planning of the energy hub has been presented in [16], in which the resiliency of energy demand is considered through the robust chance constraints method. To investigate the effect of energy storage systems on the operation of a multicarrier energy microgrid, a combined method of failure modes and effects analysis (FMEA) and the Monte Carlo method have been presented in [17], in which different strategies have been investigated for exploiting energy storage systems. Finally, in [18], a new analytical method for assessing the resiliency of CHP systems has been presented, in which the effect of energy exchange between the electrical and gas systems on system security has been investigated and the availability of the network's electricity and gas has been evaluated by the shortest path method and topology simplification approach. In a similar way [19], switching between heat supplies and electrical energy units is introduced as an approach to reduce gas usage while enhancing the security of the power system's operation. Several factors are considered, including the natural gas price, demand for electricity and gas, possible outages in natural gas pipelines, and supply failures. Weather impacts on the resiliency level of networks are discussed in [20]. In that research, a planning-targeted resilience assessment framework that considers the impact of multiple factors is established to accurately find the weak links of the transmission system and improve the system's resilience. In [21], the problem of CHP economic emission dispatch is investigated. In this regard, a two-stage approach is proposed by combining multiobjective optimization with an integrated decision-making. In such problems, a Pareto-optimal solution set could be found by using decision-making methods.

In all the reviewed articles and similar works, however, economic or reliability-based operations have been well studied. However, there are some gaps in resilient-oriented operation, thermal-electrical sections' cooperation during emergency conditions, and weather impact on hub system operation. There are few works that study both economics and resilient operations. In this regard, research gaps such as focusing on either economic or resilient aspects and defining a clear difference between reliability and resiliency are considered. In this paper, a multiobjective optimization model is proposed for the optimal performance of energy hub systems in terms of economic and resilient operations during storms and other extreme weather conditions. In this model, the total operating cost of energy hub systems, including the cost of interacting with electric, gas, and water networks and the operating costs of local energy resources, is minimized while the resiliency index, which is a function of the ENS index during high-risk periods, is maximized. The proposed model considers the objective functions, namely the total cost of the hub energy system and the electric energy not supplied, as an index for the resiliency and security of systems during storms. The main difference between the proposed method and the previous studies is the operational planning dependency on forecasted probabilistic events during short time intervals, such as outages caused by weather conditions. In this paper, using the proposed epsilon-constraint method, the multiobjective model is solved with opposite objective functions, and the Pareto optimal solutions are obtained. Each of the Pareto solutions includes operation costs and resiliency improvement actions, namely, the resiliency response program (RRP). In fact, each solution is a strategy that can be selected as a solution to the problem, depending on the expected goals.

Considering the purpose of the studied model, which is to meet economic goals and warily operation to improve resiliency, and to take into account their contradictory nature simultaneously, the max-min fuzzy method is used to establish a compromise condition between the objective functions. By implementing this method, a compromise solution that meets both objective functions is obtained. Also, the effect of providing the RRP and the participation of electric consumers in these programs on the performance of the proposed model is studied in the proposed model.

In brief, the contributions of this paper can be summarized as follows:

(i) Developing a multiobjective mathematical model to determine the optimal performance of energy hub systems in terms of economic performance and resiliency improvement simultaneously with unique operational planning for each forecasted probabilistic event that may be caused by storms.

(ii) Minimizing the total cost of energy hub systems and maximizing their resiliency, and in sequence, electric consumer welfare, are the objective functions of the problem when considering their contradiction.

(iii) Investigating the effect of RRP on the performance of the proposed model.

The rest of the paper is organized as follows: the proposed mathematical formulation of the studied model is presented in Section 2. Section 3 presents and analyzes the simulations and results. Finally, the conclusions are presented in Section 4.

2. Mathematical Formulation

In this section, the economic operation of an energy hub system is modeled as mixed-integer nonlinear programming (MINLP) by considering electric resiliency improvement under the consideration of RRP.

2.1. Objective Functions. To economically operate an energy hub system, the total cost of the system, including the cost of purchasing electric power from the upstream grid, the cost of purchasing gas from the gas network, the cost of purchasing water from the water network, and the cost of operating local energy resources, must be minimized, which is expressed in the following equation:

$$\phi 1 = \mathrm{Min}\, OC = \sum_{t=1}^{T} \left(\begin{array}{c} \lambda_t^{\mathrm{net}} \times P_t^{\mathrm{net}} + \lambda^{g} \times G_t^{\mathrm{net}} \\ + \lambda_{ST}^{h} \times \left(P_t^{c,hs} + P_t^{d,hs}\right) \\ + \lambda_{ST}^{e} \times \left(P_t^{c,es} + P_t^{d,es}\right) \\ + \lambda^{\mathrm{wind}} \times P_t^{w} + \lambda^{wr} \times Wr_t^{\mathrm{net}} \end{array} \right). \quad (1)$$

The second objective function of the studied model reflects the resiliency level of the system, which serves the function of the ENS in proportion to the total electric demand that must be maximized. The time framework for resiliency improvement in this paper is 24 hours. By considering the nature of hub systems, it is obvious that the electrical part of the system is more sensitive to weather conditions, but heat infrastructure is supported well against the weather for other physical damages. So, it is assumed that extreme weather conditions will affect electrical infrastructure [21]. This function is expressed in the following equations:

$$\phi 2 = \mathrm{Max}\, \Gamma = 1 - \frac{\mathrm{ENS}}{\sum_{t=1}^{T} L_t^{e}}, \quad (2)$$

$$\mathrm{ENS} = \sum_{t=1}^{T} LS_t^{e}, \quad (3)$$

$$0 \le LS_t^{e} \le LS_{\max}^{e} \times B_t^{LS}. \quad (4)$$

According to equation (2), the maximum value of the proposed index is expected because, in this case, the amount of ENS is minimized, which is desirable for the electrical consumers of the energy hub system in terms of resiliency. In other words, the proposed index will be maximized when the resiliency of the hub system is increased during storms and normal conditions. In equation (3), the total value of ENS is summed during operational planning. Also, in equation (4), binary nature of outages and maximum load curtailment is considered.

2.2. Technical Constraints. The balance equations for the electrical, thermal, gas, and water demands are presented in equations (5)–(8), respectively. According to the following equation, the required electric demand must be supplied by the electric power purchased from the upstream network, the CHP unit's power, the wind power production, and the output power of the electric storage system:

$$L_t^{e,DRP} + P_t^{c,es} = P_t^{\mathrm{net}} + P_t^{\mathrm{chp}} + P_t^{w} + P_t^{d,es} + LS_t^{e}. \quad (5)$$

According to the following equation, the thermal demand of the energy hub system is met by the heat production of the CHP unit, as well as the heat production of the boiler and the output heat of the thermal storage system:

$$L_t^{h} + H_t^{c,hs} = H_t^{bo} + H_t^{\mathrm{chp}} + H_t^{d,hs}. \quad (6)$$

Based on the following equation, the total gas purchased from the gas network must meet gas demand and supply CHP and boiler units:

$$L_t^{g} = G_t^{\mathrm{net}} - G_t^{bo} - G_t^{\mathrm{chp}}. \quad (7)$$

Finally, according to the following equation, the water purchased from the water network must meet the water demand of the energy hub system:

$$L_t^{w} = Wr_t^{\mathrm{net}}. \quad (8)$$

The power generated by the wind turbine, which corresponds to the hourly wind speed, is expressed as follows:

$$P_t^{w} = \begin{cases} 0, & \text{if } s_{co} < s_t < s_{ci}, \\ P_r\left(z - y \times s_t + x \times s_t^{2}\right), & \text{if } s_{ci} \le s_t < s_r, \\ P_r, & \text{if } s_r \le s_t < s_{co}. \end{cases} \quad (9)$$

The constraint of the upstream network power is presented in the following equation, based on which the generated electrical power of the upstream network should be within the nominal range.

$$0 \le P_t^{\mathrm{net}} \le P_{\max}^{\mathrm{net}}. \quad (10)$$

The power and heat produced by the CHP system, which are directly related to the gas consumed by this system, are calculated by the following equations:

$$P_t^{\mathrm{chp}} = \eta_{ge}^{\mathrm{chp}} \times G_t^{\mathrm{chp}}, \quad (11)$$

$$H_t^{\mathrm{chp}} = \eta_{gh}^{\mathrm{chp}} \times G_t^{\mathrm{chp}}. \quad (12)$$

The output of thermal energy and electric energy depend on each other by considering the operational limits for CHP, which are expressed as follows:

$$H_t^{\mathrm{chp}} = P_t^{\mathrm{chp}} \times \eta_{ge}^{\mathrm{chp}} \times HPR^{\mathrm{chp}}. \quad (13)$$

The power generation restrictions of the CHP system are expressed as follows:

$$P_{\min}^{\mathrm{chp}} \le P_t^{\mathrm{chp}} \le P_{\max}^{\mathrm{chp}}. \quad (14)$$

The heat generated by the boiler is presented by equation (15) and is constrained by equation (16).

$$H_t^{bo} = \eta^{bo} \times G_t^{bo}, \quad (15)$$

$$H_{\min}^{bo} \leq H_t^{bo} \leq H_{\max}^{bo}. \quad (16)$$

The electrical storage system is modeled by equations (17)–(21). The energy existing in the electric storage is expressed by (17) and constrained by (18).

$$P_{t+1}^{es} = P_t^{es} + P_t^{c,es} \times \eta_c^{es} - \frac{P_t^{d,es}}{\eta_d^{es}}; \forall t < 24, \quad (17)$$

$$P_{\min}^{\text{es}} \leq P_t^{\text{es}} \leq P_{\max}^{\text{es}}. \quad (18)$$

The constraints related to the charging and discharging power of the electrical storage system are expressed by the following equations:

$$P_{\min}^{c,\text{es}} \times B_t^{c,\text{es}} \leq P_t^{c,\text{es}} \leq P_{\max}^{c,\text{es}} \times B_t^{c,\text{es}}, \quad (19)$$

$$P_{\min}^{d,es} \times B_t^{d,es} \leq P_t^{d,\text{es}} \leq P_{\max}^{d,\text{es}} \times B_t^{d,es}. \quad (20)$$

The following equation is applied to isolate the charging and discharging processes:

$$B_t^{c,\text{es}} + B_t^{d,\text{es}} \leq 1. \quad (21)$$

Like the electrical storage system, a thermal storage system is used for thermal energy management in the studied energy hub system. The heat existing in the thermal storage is expressed by

$$H_{t+1}^{hs} = H_t^{hs} + H_t^{c,hs} \times \eta_c^{hs} - \frac{H_t^{d,hs}}{\eta_d^{hs}}; \forall t < 24. \quad (22)$$

The following equation is used to limit the heat existing in the thermal storage:

$$H_{\min}^{hs} \leq H_t^{hs} \leq H_{\max}^{hs}. \quad (23)$$

The input and output heat in the thermal storage are limited by the following equations:

$$H_{\min}^{c,hs} \times B_t^{c,hs} \leq H_t^{c,hs} \leq H_{\max}^{c,hs} \times B_t^{c,hs}, \quad (24)$$

$$H_{\min}^{d,hs} \times B_t^{d,hs} \leq H_t^{d,hs} \leq H_{\max}^{d,hs} \times B_t^{d,hs}. \quad (25)$$

Finally, the simultaneous charging/discharging process of the thermal storage is limited by the following equation:

$$B_t^{c,hs} + B_t^{d,hs} \leq 1. \quad (26)$$

The related restrictions of gas and water purchased from gas and water networks are expressed by the following equations:

$$G_{\min}^{\text{net}} \leq G_t^{\text{net}} \leq G_{\max}^{\text{net}}, \quad (27)$$

$$Wr_{\min}^{\text{net}} \leq Wr_t^{\text{net}} \leq Wr_{\max}^{\text{net}}. \quad (28)$$

To model the shifting electric loads, the Time of Use (TOU) model is used, based on which a portion of the electric demand is transferred from the peak interval to the non-peak intervals, and this flattens the load curve [22]. The new electric demand for the energy hub system can be expressed as follows:

$$L_t^{e,DRP} = L_t^e + P_t^{TOU,inc} - P_t^{TOU,\text{dec}}. \quad (29)$$

The amount of the transferred power in this program is limited by the following equations:

$$0 \leq P_t^{TOU,inc} \leq B_t^{TOU,inc} \times P_{\max}^{TOU,inc} \times L_t^e, \quad (30)$$

$$0 \leq P_t^{TOU,\text{dec}} \leq B_t^{TOU,\text{dec}} \times P_{\max}^{TOU,\text{dec}} \times L_t^e. \quad (31)$$

It should be noted that the electrical load cannot be increased/decreased simultaneously, which is expressed as follows:

$$B_t^{TOU,inc} + B_t^{TOU,\text{dec}} \leq 1. \quad (32)$$

Also, the total increase in load should be equal to its total reduction during the scheduling period. This is expressed as follows:

$$\sum_{t=1}^{T} B_t^{TOU,inc} = \sum_{t=1}^{T} B_t^{TOU,\text{dec}}. \quad (33)$$

Results of different studies show that extreme weather conditions (e.g., storms) are the main reason for more than half of the faults in electrical grids [23]. To evaluate how a resilient grid modifies operational scheduling by considering weather conditions, outages are distinguished into two classes. In the first class, outages caused by nonweather reasons are modeled by a constant interruption value. In the second class, weather-caused faults are considered. To have a proper analysis to evaluate the effect of weather conditions on outage rate, the faults mentioned in the second class are modeled by correlations as presented in [23]. Unfortunately, standard distribution test systems do not' have weather-caused event data, so real, normalized data are used in simulations to evaluate a resilience grid's behavior during different weather conditions. In [23], the correlation between events and wind speed for short-time intervals is modeled as follows [23]:

$$N_w = 0.0012W^2 - 0.0131W. \quad (34)$$

It is assumed that average wind speed probability could be predicted in one-hour time intervals. This paper uses average wind speed for all time intervals. Wind speed affects the number of outages. It is clear that wind flow patterns and wind speed profiles change over time, and it is possible to estimate some wind patterns for each area.

2.3. Multiobjectives Optimization Model. A two-objective optimization model is devoted to the problem, in which several objective functions are simultaneously optimized. Several methods have been developed and applied to solve such problems. One of the most common and most effective examples of these methods is the epsilon-constraint method [24–26]. Since optimized objective functions in multiobjective problems are usually in conflict with each other, there must be a compromise condition between them, which is carried out by the max-min fuzzy method [27, 28]. In this section, the methods mentioned above are applied and explained step-by-step.

Based on the epsilon-constraint method, one of the objective functions (the cost function in this paper), which is more prioritized than another, is selected as the base or main purpose function. Then, the second objective function (the resiliency index function in this paper), which is varied by the epsilon factor from its minimum value to its maximum value, is considered to be a constraint for the base objective function. Thus, the two-objective optimization model becomes a one-objective optimization problem:

$$\begin{aligned} &\mathrm{OF} = \operatorname{Min} OC, \\ &\Gamma \leq \varepsilon, \\ &\text{All constraints.} \end{aligned} \tag{35}$$

The next step is to determine the compromise condition between the cost function and the resiliency index function using the max-min fuzzy method. Since the nature of the objective functions studied in this article is not the same, their per-unit quantities must be calculated. To this end, the following equation is used:

$$OC^n_{pu} = \begin{cases} 1, & \text{if } OC^n \leq OC^{\min}, \\ \dfrac{OC^{\max} - OC^n}{OC^{\max} - OC^{\min}}, & \text{if } OC^{\min} \leq OC^n \leq OC^{\max}, \\ 0, & \text{if } OC^n \geq OC^{\max}, \end{cases}$$

$$\Gamma^n_{pu} = \begin{cases} 1, & \text{if } \Gamma^n \leq \Gamma^{\min}, \\ \dfrac{\Gamma^{\max} - \Gamma^n}{\Gamma^{\max} - \Gamma^{\min}}, & \text{if } \Gamma^{\min} \leq \Gamma^n \leq \Gamma^{\max}, \\ 0, & \text{if } \Gamma^n \geq \Gamma^{\max}, \end{cases} \tag{36}$$

The next step is to compare the per-unit quantities of the objective functions in each repetition to determine the minimum value between the two objective functions in each repetition:

$$\mu^n_{pu} = \operatorname{Min}\left(OC^n_{pu}, \Gamma^n_{pu}\right). \tag{37}$$

The final step is to select the highest value between the minimum values selected in the previous step. This solution is the compromise solution to the studied problem. Also, the software of the general algebraic modeling system (GAMS) is used to solve the problem.

$$\mu^{\max}_{pu} = \operatorname{Max}\left(\mu^1_{pu}, \ldots\ldots, \mu^N_{pu}\right). \tag{38}$$

3. Simulation and Numerical Results

In this section, the optimal performance of the energy hub system, as shown in Figure 1, is numerically studied under an MINLP considering the operation cost and the resiliency index as objective functions, and the output results are presented.

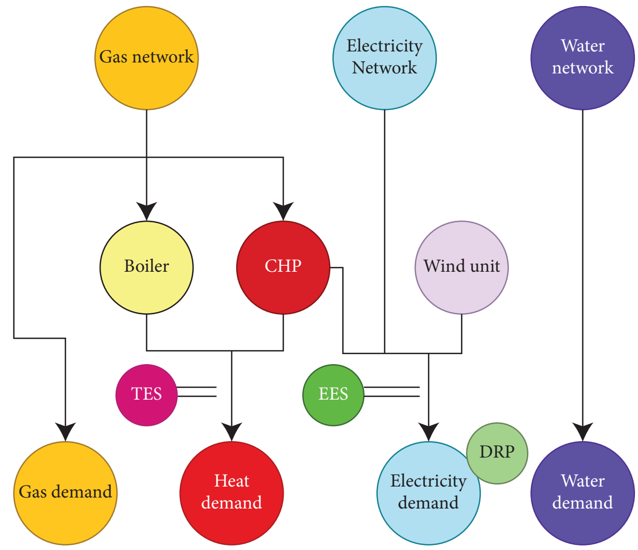

Figure 1: The studied energy hub system.

3.1. Simulation Input Parameters. The input parameters used in the simulations are presented in this section. The energy hub system must be responsive to four different electrical, thermal, gas, and water demands, as illustrated in Figures 2–5, respectively. The proposed method could be used for various systems with different time intervals. In other words, there is no limitation for size or time steps.

The price of the upstream network is presented in Figure 6. It should be noted that the cost of gas and water purchased from the gas and water networks is 6 ¢/m^3 and 4 ¢/ton, respectively. It is necessary to mention that these parameters were extracted from similar works and their values are the same or near to those of related papers [29–31]. The hourly wind speed is presented in Figure 7.

The technical parameters of the electrical and thermal storage systems are presented in Tables 1 and 2. The technical parameters for the upstream, gas, and water networks are presented in Table 3. The technical data of the local units of the energy hub system are presented in Table 4. The costs of the operation of local units are presented in Table 5. It is necessary to mention that these parameters were extracted from similar works and their values are the same or near to those in related papers [29–31]. It should be noted that the maximum constraint for increasing/decreasing the electrical load in the demand response program (DRP) is considered 20% of the base load.

To investigate the proposed method for resiliency improvement during storms, it is assumed that wind speed is variable, as presented in Figure 7. Also, as mentioned before, it is assumed that extreme weather conditions will affect the electrical part of the system due to its design and status. The physical effect of extreme weather conditions on the thermal part is negligible; however, operational planning of the hub

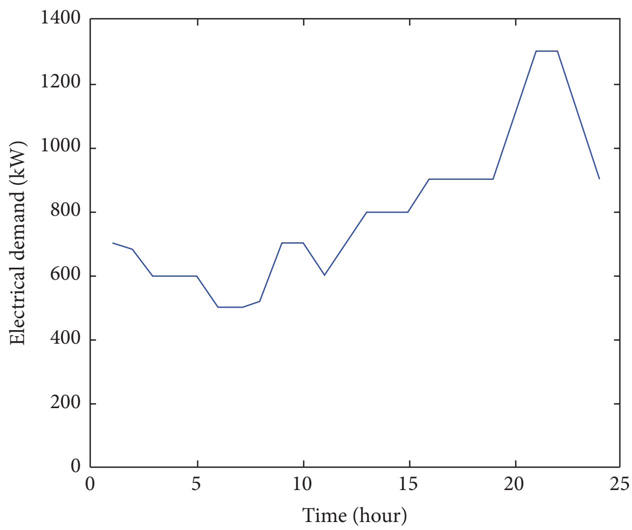

Figure 2: Electrical demand of the energy hub system.

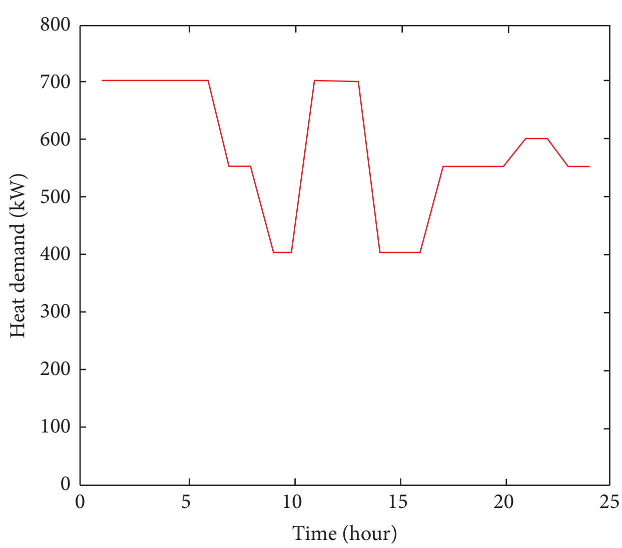

Figure 3: Thermal demand of the energy hub system.

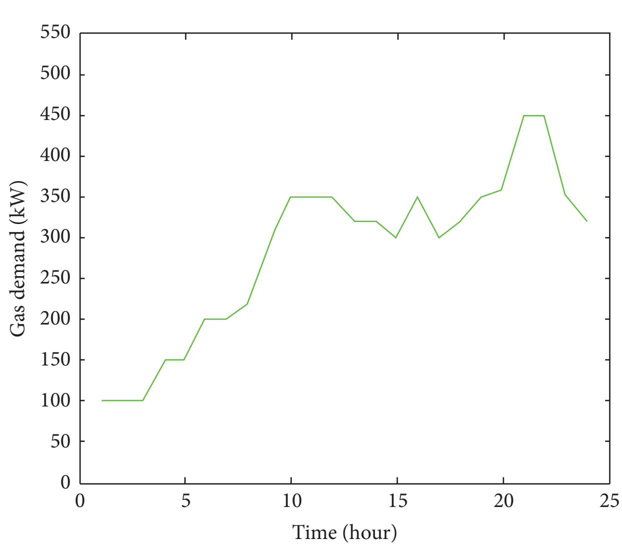

Figure 4: Gas demand of the energy hub system.

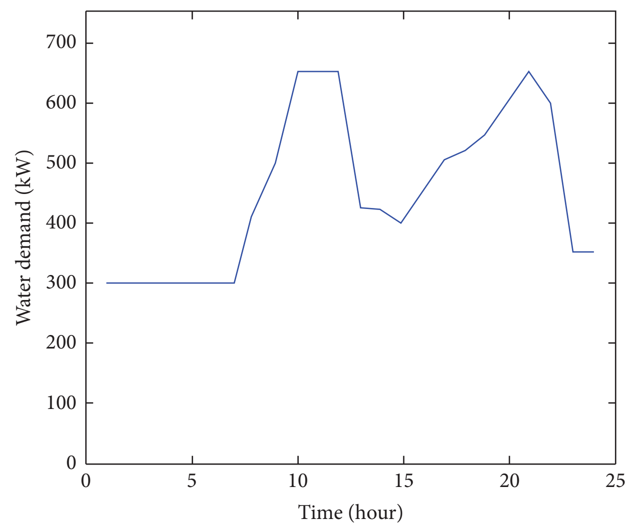

Figure 5: Water demand of the energy hub system.

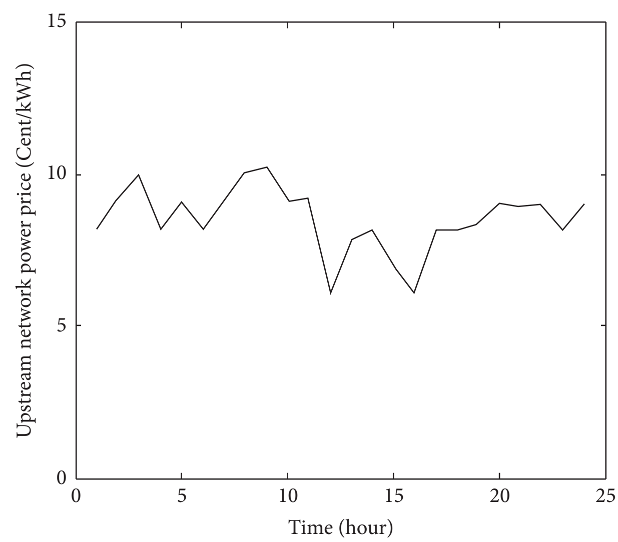

Figure 6: Price of the upstream network.

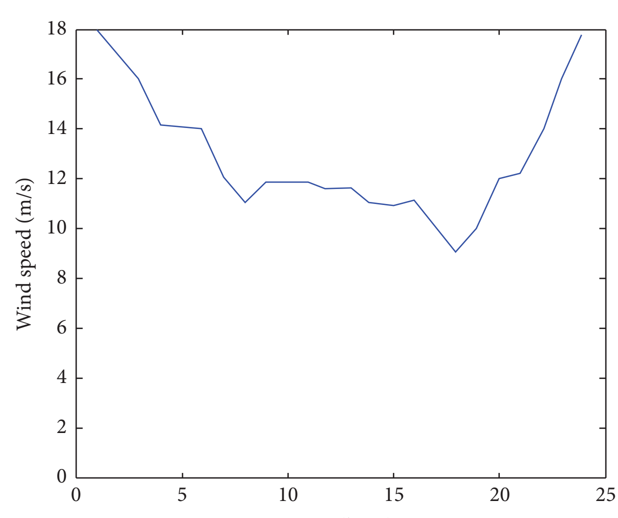

Figure 7: Wind speed.

TABLE 1: Technical parameters of the electrical storage system.

Electrical storage systems		
#	Unit	Value
$P^{es}_{\min}$	kWh	15
$P^{es}_{\max}$	kWh	270
$P^{c,es}_{\min}$	kW	15
$P^{c,es}_{\max}$	kW	270
$P^{d,es}_{\min}$	kW	15
$P^{d,es}_{\max}$	kW	270
η^{es}_{c}	%	90
η^{es}_{d}	%	90

TABLE 2: Technical parameters of the thermal storage system.

Thermal storage systems		
#	Unit	Value
$H^{hs}_{\min}$	kWh	10
$H^{hs}_{\max}$	kWh	180
$H^{c,hs}_{\min}$	kW	10
$H^{c,hs}_{\max}$	kW	180
$H^{d,hs}_{\min}$	kW	10
$H^{d,hs}_{\max}$	kW	180
η^{hs}_{c}	%	90
η^{hs}_{d}	%	90

TABLE 3: Technical parameters of the upstream, gas, and water networks.

Upstream, gas, and water networks		
#	Unit	Value
$Wr^{\text{net}}_{\min}$	Ton	0
$Wr^{\text{net}}_{\max}$	Ton	1000
$G^{\text{net}}_{\min}$	m^3	0
$G^{\text{net}}_{\max}$	m^3	1800
$P^{\text{net}}_{\max}$	kW	1000

TABLE 4: Technical information of the local units.

CHP and boiler units			Wind units		
#	Unit	Value	#	Unit	Value
η^{chp}_{ge}	%	40	P_r	kW	400
η^{chp}_{gh}	%	35	x, y, z	—	0.07, 0.01, 0.03
$P^{chp}_{\min}$	kW	0	s_r	m/s	10
$P^{chp}_{\max}$	kW	800	s_{ci}	m/s	4
η^{bo}	%	85	s_{co}	m/s	22
$H^{bo}_{\min}$	kW	0	—	—	—
$H^{bo}_{\max}$	kW	800	—	—	—

TABLE 5: Cost of the operation of the local units.

#	Unit	Value
λ^{g}	Cent/kWh	6
λ^{wr}	Cent/kWh	4
λ^{wind}	Cent/kWh	0
λ^{e}_{ST}	Cent/kWh	2
λ^{h}_{ST}	Cent/kWh	2

system in both electrical and thermal parts will be affected. Operational planning of the electrical part of the system during storms will be affected by considering the effects of wind speed on the outage rate of lines [23]. Wind speed in crescent in certain hours increases the probability of the line outage and in sequence, the ENS amount is increased. This fact is modeled by adding a value to the outage rate of lines calculated by (34) for each hour. ENS indicates the resiliency of the grid against extreme weather conditions. Also, the ENS penalty cost changes the operational cost of the hub system due to the dependency of electrical and thermal parts on each other. To improve the resiliency and economic operation of the hub system, some actions, such as changes in CHP outputs, power purchase from the upstream grid, scheduling of storage, and demand response programs, are rescheduled due to the storm effect on the outage rate of lines. In this paper, all actions to improve the resiliency of the system are referred to as RRPs. The optimization problem is MINLP. So, simulations are carried out in GAMS software due to the nature of the problem.

To investigate the proposed operational planning method, two different cases are considered as follows:

Case 1: operational planning in the case that the system operator makes decisions to improve resiliency (RRP without DRP).

Case 2: operational planning in the case that both the system operator and consumers cooperate to improve resiliency (RRP with DRP).

By performing related simulations in different states, the optimal Pareto solutions are obtained in different cases. The used computing system was a Core i5-2.40 GHz with 8 GB of RAM on a 64-bit system and total runtime for cases was 5–10 seconds. The Pareto solutions with/without DRP are presented in Figure 8. According to the results obtained in Figure 8, on the one hand, the operation cost of the system will be \$1983.876 if the objective function includes only the cost function of the energy hub system. In this case, the resiliency index will be equal to 60.9%. On the other hand, considering the resiliency index as the objective function, the operation cost of the system is \$2589.028 and the resiliency index is equal to 1 or 100%. These results are part of the optimal Pareto solutions that can be achieved depending on different expectations. Using the max-min fuzzy method, solution #11 will be chosen as the compromise solution, according to which the system operation cost is \$2279.190 and the resiliency index is equal to 0.815 or 81.5%, respectively. According to Figure 8, on the one hand, considering the cost function as the objective function under DRP, the operation cost of the system is \$1949.808 and the resiliency index is equal to 0.600. On the other hand, considering the resiliency index as an objective function, the resiliency index is equal to 100%, and the cost of the system is \$2567.441. By providing the compromise condition between the objective functions, the system operating cost and the resiliency index would be \$2258.173 and 81.1%, respectively.

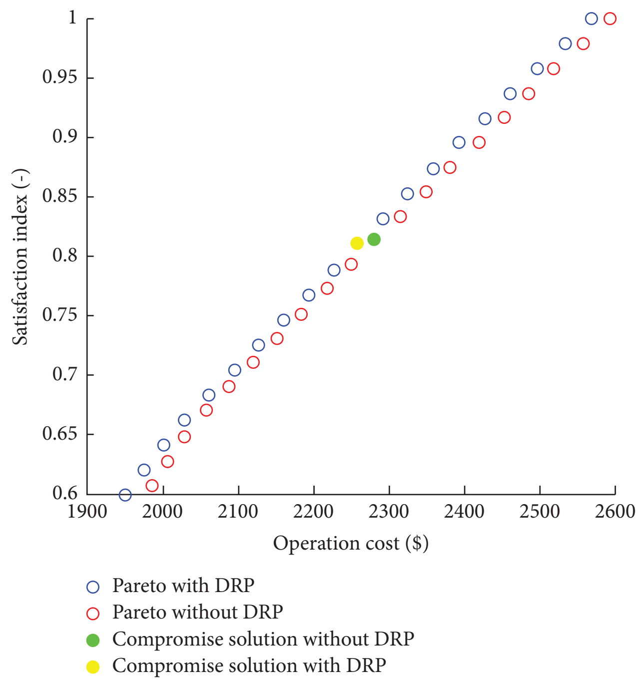

Figure 8: Pareto solutions with/without DRP.

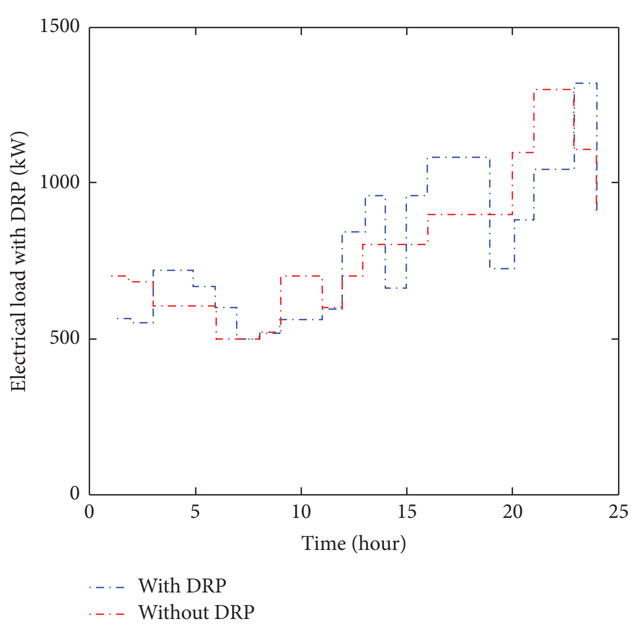

Figure 9: Electric load with/without DRP.

By comparing these results, it can be observed that the contribution of shifting load in DRP has caused the operation cost of the system to be reduced by $21.017, equivalent to 0.9221%, in comparison with the condition that there is no contribution of shifting load. In other words, DRP has a positive effect on RRP efficiency. This amount of reduction is desirable for the resilient operation of the energy hub system from an economic point of view. In order to see the effect of providing RRP on the load profile, the electric load of the energy hub system with/without the possibility of participating in DRP is presented in Figure 9.

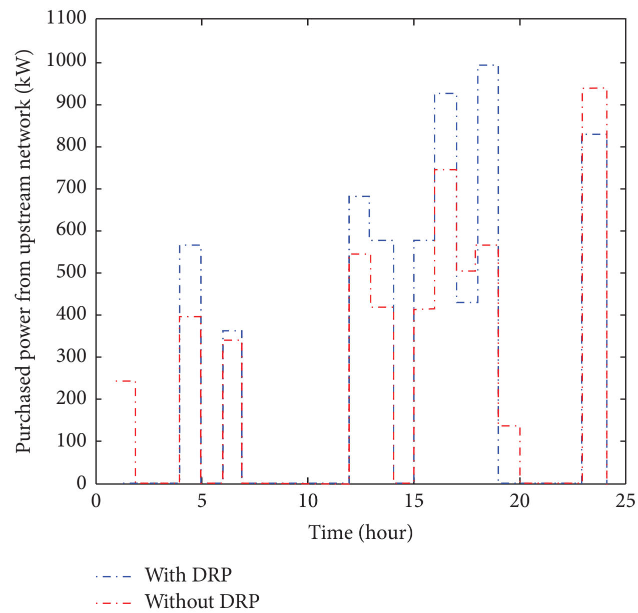

Figure 10: Power purchased from the upstream network.

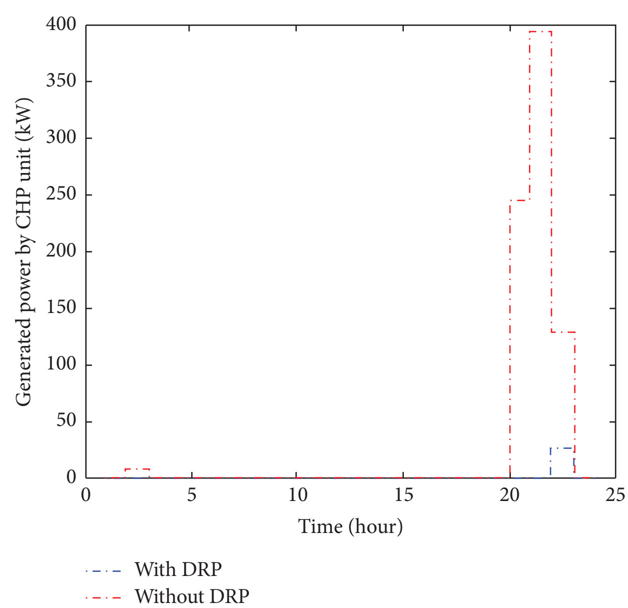

Figure 11: Generated power by CHP unit.

To supply the above electrical load with/without consumer cooperation, the energy hub system has purchased power from the upstream network. The related profile of the purchased power is presented in Figure 10. It is worth noting that the purchased power in the presence of DRP is appropriate to the new profile of the load under this program, which can affect the operating cost of the hub system and resiliency index due to the hourly cost of electricity. In other words, not only the price of upstream networks changes the purchase profile, but also outages amount based on wind speed affects it.

In addition to the power of the upstream network, the power generated by CHP units also contributes to the energy hub system's ability to provide the electrical load. Its related

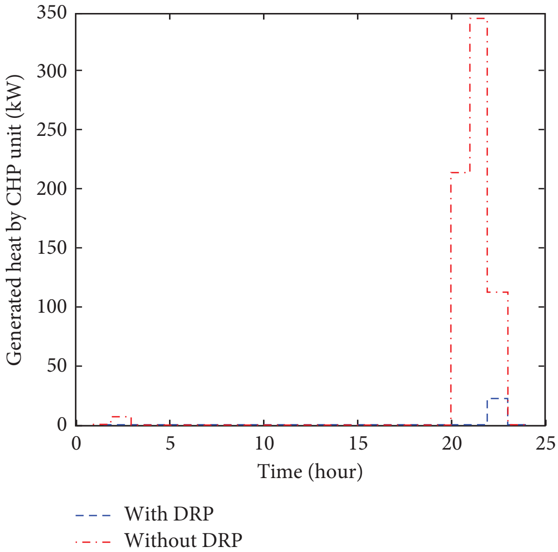

FIGURE 12: Generated heat by the CHP unit.

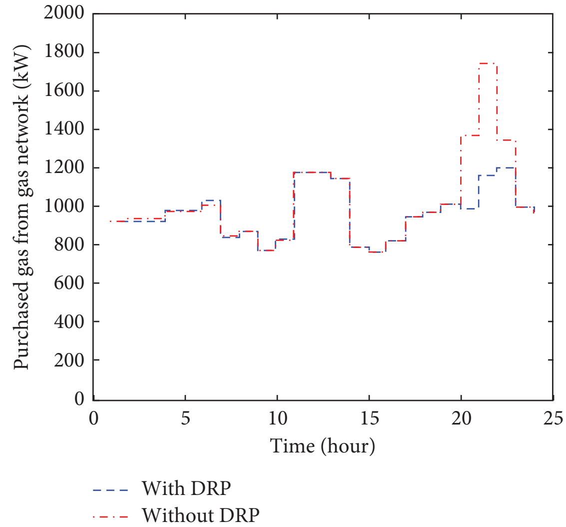

FIGURE 14: The gas purchased from the gas network.

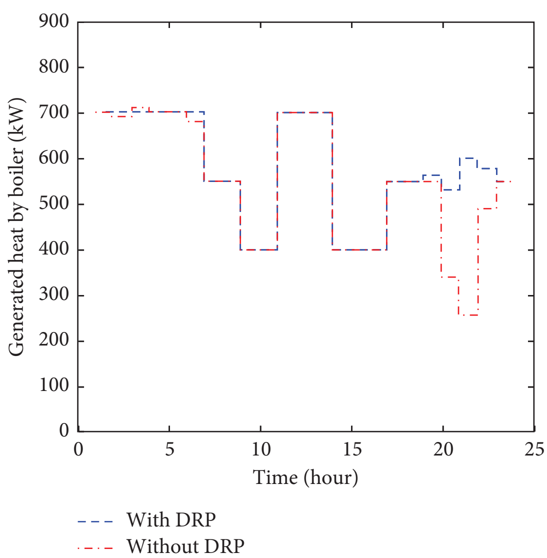

FIGURE 13: The heat generated by the boiler.

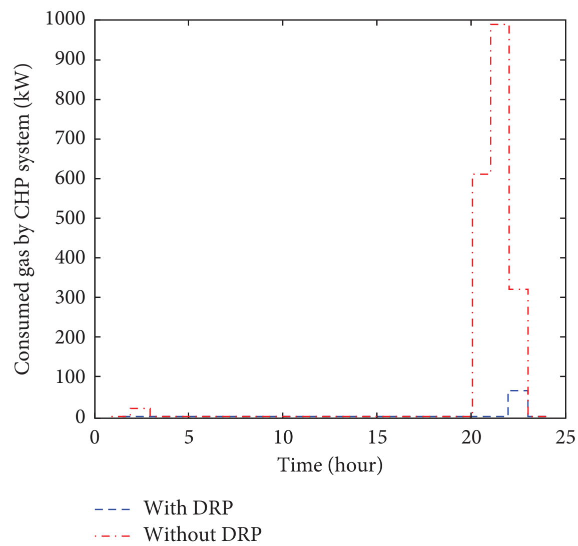

FIGURE 15: The gas consumed by CHP.

profile is displayed in Figure 11. Regarding the relationship between power and heat generated by CHP (13), the heat generated by this unit for supplying the thermal energy of the energy hub system is presented in Figure 12. It is clear that DRP, by considering resiliency improvement, can change the power and heat generated by CHP sharply. In addition to the CHP unit, the boiler unit also plays an important role in supplying the heat load of the energy hub system. Due to the structure of thermal units and the efficiencies of local units, most of the thermal load of the energy hub system is provided by the boiler unit, which is a unit specific to heat production. The heat generated by this unit is presented in Figure 13.

To operate the energy generated through the above-mentioned units (CHP unit and boiler unit), gas purchased from the gas network is consumed to the desired extent by these units. The total gas purchased from the gas network, along with the gas consumed by the CHP unit and boiler unit, is presented in Figures 14–16. To optimally use the power and heat generated in the energy hub system, electrical and thermal storage systems were applied to contribute to the efficiency of the energy hub system from the point of view of resiliency and economic performance by saving energy timely and consuming it in the proper hours. The charging and discharging power of the electrical storage system, as well as its existing energy, are presented in Figures 17 and 18. Also, the input and output heat of the heat

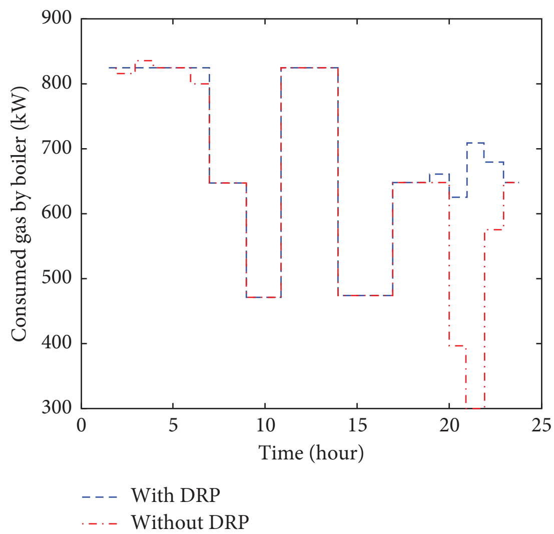

Figure 16: The gas consumed by the boiler.

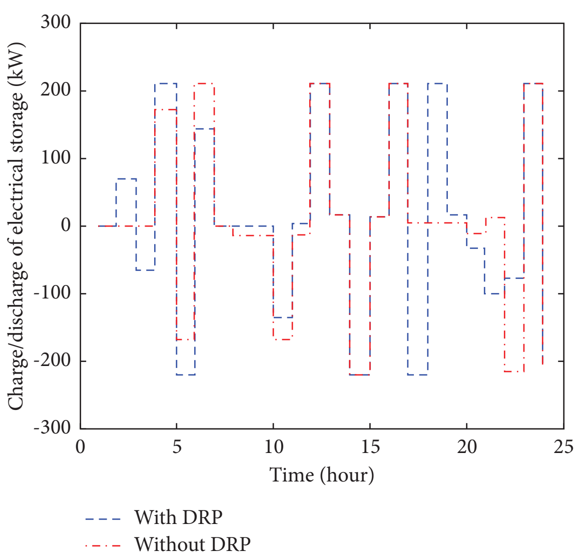

Figure 17: Charge and discharge of the electrical storage.

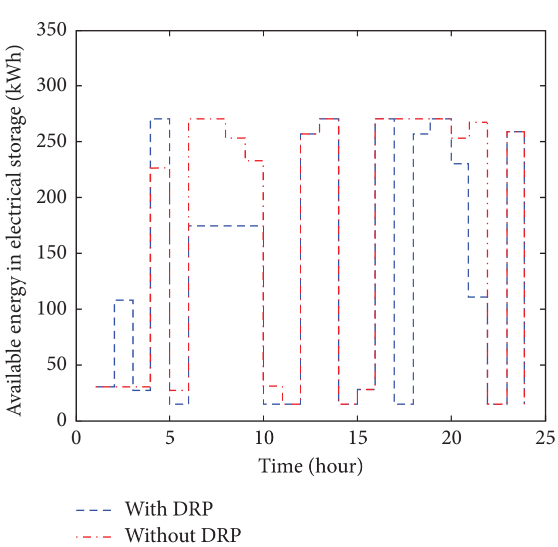

Figure 18: The energy stored in the electrical storage.

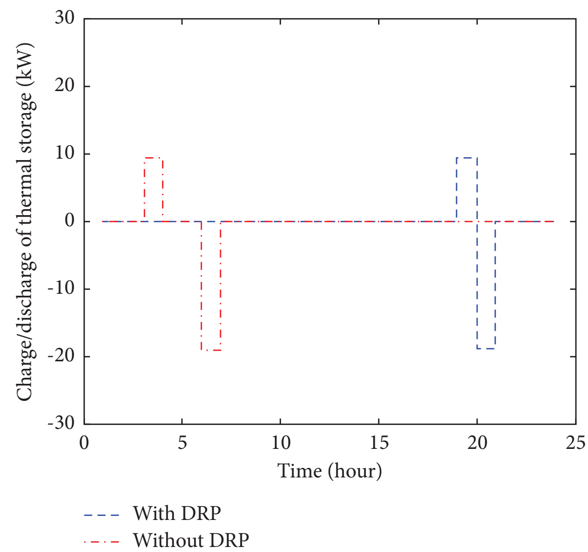

Figure 19: Charge and discharge of the thermal storage.

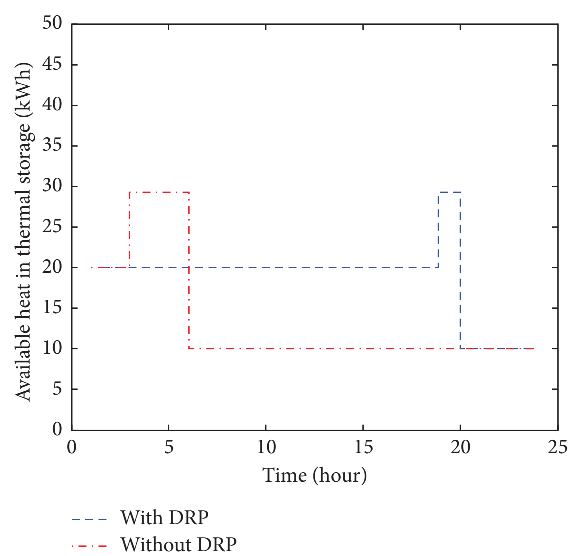

Figure 20: The heat stored in thermal storage.

storage system, along with the heat stored in it, are presented in Figures 19 and 20.

4. Conclusions

In this paper, the concept of an energy hub system is used to supply electric, thermal, gas, and water loads. Energy transformations in these systems allow for the optimal supply of energy loads and bring about the lowest operation costs and the highest level of resiliency. Furthermore, in this paper, a multiobjective optimization model for the economic performance of the energy hub system and the resiliency of electrical consumers is presented, in which the total operating cost of the system is minimized and the consumer resiliency index as a function of ENS is maximized. Applying the epsilon-constraint method, the proposed model with/without taking into account the possibility of electric consumer participation in DRP is solved and Pareto solutions are obtained. Then, by applying the max-min fuzzy method, the compromise solution is selected among the Pareto solutions. Results proved that the proposed RRP improved resiliency and reduced operational costs at the same time. In this regard, simulation results showed that using RRP (with/without) could improve the resiliency index with a logical increase in operational cost. According to the results, in PPR without DRP, the resiliency index could reach its maximum possible value (a 64.2% improvement), while the operational cost will increase by up to 30.5%. Also, the optimal balance could be obtained when the resiliency index enhances by 33.8% with an extra operational cost of 14.9%. According to the results, it can be seen that economic performance improves while the resiliency index declines under the condition that DRP is considered. In the proposed method (RRP including DRP), in order to get the maximum available resiliency index (66.7% more than in a pure economic operation), the operational cost of the system was increased by 31.7%. Also, in optimal resilient-economic balance, values of the resiliency index are enhanced by 35.2% with a 15.8% increment in operational cost. These results proved that simultaneous economic-resilient operation could be different with pure economic or resilient operations. Also, based on the risk level, it could be more closed for both operation methods. This fact can affect the priorities of planning and the participation of consumers in RRP services. In future work, the relationship between various risk levels and changes in operation could be investigated by considering more detailed models of hub energy systems, heat/power convertors, and uncertainties of demand/price.

Symbols

Functions

$\phi 1$: The first objective function in the two-objective optimization problem
$\phi 2$: The second objective function in the two-objective optimization problem
OF: Objective function of the single-objective optimization problem

Indices

t: Time index
n: Index of Epsilon-constraint method repetition
ε: Epsilon factor
λ_t^{net}: Network power price
λ^g: Gas price
λ_{ST}^h: Operation cost of the thermal storage
λ_{ST}^e: Operation cost of the electrical storage
λ^{wind}: Operation cost of the wind generator
λ^{wr}: Water network cost
η_{ge}^{chp}: Electricity efficiency of the combined heat and power (CHP)
η_{gh}^{chp}: CHP unit thermal efficiency
η_{he}^{chp}: Efficiency of the heat exchanger
η^{bo}: Boiler efficiency
η_c^{es}: Electric storage charging efficiency
η_d^{es}: Electric storage discharging efficiency
η_c^{hs}: Charging efficiency of the thermal storage
η_d^{hs}: Thermal storage charging efficiency
η_d^{hs}: Thermal storage discharging efficiency
$G_{\min}^{\text{net}}$: Minimum constraint of gas purchased from the upstream network
$G_{\max}^{\text{net}}$: Maximum constraint of gas purchased from the upstream network
$H_{\min}^{bo}$: Minimum constraint of thermal energy generated by the boiler
$H_{\max}^{bo}$: Maximum constraint of thermal energy generated by the boiler
$H_{\min}^{hs}$: Minimum constraint of heat existing in the thermal storage
$H_{\max}^{hs}$: Maximum constraint of heat existing in the thermal storage
$H_{\min}^{c,hs}$: Minimum constraint of heat input of the thermal storage
$H_{\max}^{c,hs}$: Maximum constraint of heat input of the thermal storage
$H_{\min}^{d,hs}$: Minimum constraint of heat output of the thermal storage
$H_{\max}^{d,hs}$: Maximum constraint of heat output of the thermal storage
HPR^{chp}: Heat to power ratio of CHP
L_t^e: Electric load of the energy hub system
L_t^h: Thermal load of the energy hub system
L_t^g: Gas load of the energy hub system
L_t^w: Water load of the energy hub system
$\text{LS}_{\max}^e$: Maximum constraint of power outage
N: Number of repetitions in the epsilon-constraint method
N_w: Number of outages caused by wind speed
P_r: Nominal power of the wind system
$P_{\max}^{\text{net}}$: Nominal power of the upstream network
$P_{\min}^{chp}$: Minimum constraint of power generated by the CHP unit
$P_{\max}^{chp}$: Maximum constraint of power generated by the CHP unit
$P_{\min}^{es}$: Minimum constraint of energy existing in the electrical storage
$P_{\max}^{es}$: Maximum constraint of energy existing in the electrical storage
$P_{\min}^{c,es}$: Minimum constraint of charging power of the electrical storage
$P_{\max}^{c,es}$: Maximum constraint of charging power of the electrical storage
$P_{\min}^{d,es}$: Minimum constraint of discharging power of the electrical storage
$P_{\max}^{d,es}$: Maximum constraint of discharging power of the electrical storage
$P_{\max}^{\text{TOU,inc}}$: Maximum constraint of shifting load (increase)
$P_{\max}^{\text{TOU,dec}}$: Maximum constraint of shifting load (decrease)
s_t: Wind speed
s_{co}: Cut-out wind speed
s_{ci}: Cut-in wind speed
s_r: Nominal wind speed

T: Number of scheduling hours
x: The coefficient applied in wind system model
W: Average wind speed
$Wr_{\min}^{\text{net}}$: Minimum constraint of water purchased from water network
$Wr_{\max}^{\text{net}}$: Maximum constraint of water purchased from water network
y: The coefficient applied in wind system model
z: The coefficient applied in wind system model

Variables

$\Gamma^{\max}$: Maximum welfare index quantity
$\Gamma^{\min}$: Minimum welfare index quantity
μ_{pu}^{n}: The minimum selected solution amount among the objective functions in each iteration
$\mu_{pu}^{\max}$: The maximum value among the selected minimums in the max-min fuzzy method
Γ: Welfare index
Γ^{n}: Welfare index in each iteration
Γ_{pu}^{n}: Per unit amount of welfare index in each iteration
ENS: Energy not supplied
G_t^{bo}: Gas consumed by the boiler
G_t^{chp}: Gas consumed by the CHP unit
G_t^{net}: Gas purchased from the gas network
H_t^{hs}: Heat stored in the thermal storage
H_t^{bo}: Amount of heat available in the boiler
H_t^{chp}: Amount of heat available in the CHP
LS_t^{e}: Loss load
$L_t^{e,DRP}$: The electric load of the energy hub system taking into account the shifting loads
$H_t^{c,hs}$: Heat input of the thermal storage
$H_t^{d,hs}$: Heat output of the thermal storage
$OC^{\max}$: The maximum operation cost of the energy hub system
$OC^{\min}$: The maximum operation cost of the energy hub system
OC: Operation cost of the energy hub system
OC^{n}: Operation cost of the energy hub system in each iteration
OC_{pu}^{n}: Per unit amount of operation cost of the energy hub system in each iteration
P_t^{chp}: Energy available in the CHP
P_t^{net}: Power purchased from the upstream network
P_t^{es}: Energy available in the electrical storage
$P_t^{c,es}$: Charging power of the electrical storage
$P_t^{d,es}$: Discharging power of the electrical storage
$P_t^{c,hs}$: Charging power of the heat storage
$P_t^{d,hs}$: Discharging power of the heat storage
P_t^{w}: Wind system power
$P_t^{TOU,inc}$: Increased load in time-of-use (TOU)
$P_t^{TOU,\text{dec}}$: Load decreased in the TOU plan
Wr_t^{net}: Purchased water from the water network

Binary Variables

$B_t^{TOU,inc}$: Binary variable of increasing load in TOU
$B_t^{TOU,\text{dec}}$: Binary variable of decreasing load in TOU
B_t^{LS}: Binary variable of outage of load
$B_t^{c,es}$: Binary variable of charging electrical storage
$B_t^{d,es}$: Binary variable of discharging electrical storage
$B_t^{c,hs}$: Binary variable of charging thermal storage
$B_t^{d,hs}$: Binary variable of discharging thermal storage.

Data Availability

The data used to support the findings of this study are available from the corresponding author upon request.

Conflicts of Interest

The authors declare that there are no conflicts of interest.

References

[1] B. Kazemi, A. Kavousi-Fard, M. Dabbaghjamanesh, and M. Karimi, "IoT-enabled operation of multi energy hubs considering electric vehicles and demand response," *IEEE Transactions on Intelligent Transportation Systems*, vol. 11, pp. 1–9, 2022.

[2] A. Malekijavan, M. Aslinezhad, and H. Zaferani, "Reliability-based operation in energy hubs with several energy networks," *Journal of Industrial Electronics, Control and Optimization Journal*, vol. 4, no. 4, pp. 433–444, 2021.

[3] S. Esmaeili, A. Anvari-Moghaddam, E. Azimi, A. Nateghi, and J. Ps Catalão, "Bi-level operation scheduling of distribution systems with multi-microgrids considering uncertainties," *Multidisciplinary Digital Publishing Institute*, vol. 9, p. 1441, 2020.

[4] X. Zhang, L. Che, M. Shahidehpour, A. S. Alabdulwahab, and A. Abusorrah, "Reliability-based optimal planning of electricity and natural gas interconnections for multiple energy hubs," *IEEE Transactions on Smart Grid*, vol. 8, no. 4, pp. 1658–1667, 2017.

[5] S. Moradi, R. Ghaffarpour, A. M. Ranjbar, and B. Mozaffari, "Optimal integrated sizing and planning of hubs with mid-size/large CHP units considering reliability of supply," *Energy Conversion and Management*, vol. 148, no. 2, pp. 974–992, 2017.

[6] Y. Lei, K. Hou, Y. Wang et al., "A new reliability assessment approach for integrated energy systems: using hierarchical decoupling optimization framework and impact-increment based state enumeration method," *Applied Energy*, vol. 210, pp. 1237–1250, 2018.

[7] H. Shahsavari, A. Nateghi, A. Safari, and E. Azimi Bizaki, "Dynamically modelling and locating solid oxide fuel cells and optimally designing fuzzy stabilisers for multi-machine system," *International Journal of Ambient Energy*, vol. 43, no. 1, pp. 4010–4019, 2021.

[8] Y. Wen, D. AlHakeem, P. Mandal et al., "Performance evaluation of probabilistic methods based on bootstrap and quantile regression to quantify PV power point forecast uncertainty," *IEEE Transactions on Neural Networks and Learning Systems*, vol. 31, no. 4, pp. 1134–1144, April 2020.

[9] M. N. Ambia, K. Meng, W. Xiao, and Z. Y. Dong, "Nested Formation approach for networked microgrid self-healing in islanded mode," *IEEE Transactions on Power Delivery*, vol. 36, no. 1, pp. 452–464, 2021.

[10] Y. Song, Y. Liu, R. Wang, and M. Ming, "Multi-objective configuration optimization for isolated microgrid with shiftable loads and mobile energy storage," *IEEE Access*, vol. 7, no. 2, pp. 95248–95263, 2019.

[11] R. Carli, G. Cavone, T. Pippia, B. De Schutter, and M. Dotoli, "Robust optimal control for demand side management of multi-carrier microgrids," *IEEE Transactions on Automation Science and Engineering*, vol. 19, no. 3, pp. 1338–1351, 2022.

[12] F. Luo, W. Kong, G. Ranzi, and Z. Y. Dong, "Optimal home energy management system with demand Charge tariff and appliance operational dependencies," *IEEE Transactions on Smart Grid*, vol. 11, no. 1, pp. 4–14, Jan. 2020.

[13] M. Paktinat, M. Amirahmadi, M. Tolou-Askari, and F. Mousavizadeh, "Optimal resilient operation of hub energy system considering uncertain parameters," *Sustainable Energy, Grids and Networks*, vol. 30, Article ID 100618, 2022.

[14] D. Araujo, N. Batista, P. Carvalho et al., "Renewable hybrid systems: characterization and tendencies," *IEEE Latin America Transactions*, vol. 18, no. 01, pp. 102–112, January 2020.

[15] S. Senemar, A. R. Seifi, M. Rastegar, and M. Parvania, "Probabilistic optimal dynamic planning of onsite solar generation for residential energy hubs," *IEEE Systems Journal*, vol. 14, no. 1, pp. 832–841, 2020.

[16] Y. Cao, W. Wei, J. Wang, S. Mei, M. Shafie-khah, and J. P. S. Catalao, "Capacity planning of energy hub in multi-carrier energy networks: a data-driven robust stochastic programming approach," *IEEE Transactions on Sustainable Energy*, vol. 11, pp. 3–14, 2020.

[17] S. Ge, H. Sun, H. Liu, J. Li, X. Zhang, and Y. Cao, "Reliability evaluation of multi-energy microgrids: energy storage devices effects analysis," *Energy Procedia*, vol. 158, no. 2, pp. 4453–4458, 2019.

[18] Q. Zhao, Y. Du, T. Zhang, and W. Zhang, "Resilience index system and comprehensive assessment method for distribution network considering multi-energy coordination," *International Journal of Electrical Power & Energy Systems*, vol. 133, Article ID 107211, December 2021.

[19] C. Juanwei, Y. Tao, X. Yue, C. Xiaohua, Y. Bo, and Z. Baomin, "Fast analytical method for reliability evaluation of electricity-gas integratedenergy system considering dispatch strategies," *Applied Energy*, vol. 242, pp. 260–272, 2019.

[20] R. Yang and Y. Li, "Resilience assessment and improvement for electric power transmission systems against typhoon disasters: a data-model hybrid driven approach," *Energy Reports*, vol. 8, pp. 10923–10936, 2022.

[21] Y. Li, J. Wang, D. Zhao, G. Li, and C. Chen, "A two-stage approach for combined heat and power economic emission dispatch: combining multi-objective optimization with integrated decision making," *Energy*, vol. 162, pp. 237–254, 2018.

[22] T. Liu, D. Zhang, S. Wang, and T. Wu, "Damping controller design based on FO-PID-EMA in VSC HVDC system to improve stability of hybrid power system," *Energy Conversion and Management*, vol. 182, pp. 126–142, 2019.

[23] B. Yousefi-khangah, S. Ghassemzadeh, S. H. Hosseini, and B. Mohammadi-Ivatloo, "Short-term scheduling problem in smart grid considering reliability improvement in bad weather conditions," *IET Generation, Transmission & Distribution*, vol. 11, no. 10, pp. 2521–2533, 2017.

[24] M. Nazari-Heris, S. Abapour, and B. Mohammadi-Ivatloo, "Optimal economic dispatch of FC-CHP based heat and power micro-grids," *Applied Thermal Engineering*, vol. 114, pp. 403–417, 2020.

[25] A. Esmaeel Nezhad, A. Ahmadi, M. S. Javadi, and M. Janghorbani, "Multi-objective decision-making framework for an electricity retailer in energy markets using lexicographic optimization and augmented epsilon-constraint," *International Transactions on Electrical Energy Systems*, vol. 25, no. 12, pp. 3660–3680, 2015.

[26] O. M. Babatunde, J. L. Munda, and Y. Hamam, "A Comprehensive State-Of-The-Art Survey on Hybrid Renewable Energy System Operations and Planning," *IEEE Access*, vol. 8, 2020.

[27] P. Wei, F. He, L. Li, X. Shi, and R. Simoes, "Multi-objective problem based operation and emission cots for heat and power hub model through peak load management in large scale users," *Energy Conversion and Management*, vol. 171, no. 2, pp. 411–426, 2018.

[28] Y. Sun, J. Xu, G. Lin, F. Ni, and R. Simoes, "An optimal performance based new multi-objective model for heat and power hub in large scale users," *Energy*, vol. 161, pp. 1234–1249, 2018.

[29] J. Najafi, A. Peiravi, A. Anvari-Moghaddam, and J. M. Guerrero, "Power-heat generation sources planning in microgrids to enhance resilience against islanding due to natural disasters," *IEEE 28th International Symposium on Industrial Electronics (ISIE)*, vol. 27, pp. 2446–2451, 2019.

[30] D. Xu, Q. Wu, B. Zhou, C. Li, L. Bai, and S. Huang, "Distributed multi-energy operation of coupled electricity, heating, and natural gas networks," *IEEE Transactions on Sustainable Energy*, vol. 11, no. 4, pp. 2457–2469, 2020.

[31] F. Jafari, H. Samet, A. R. Seifi, and M. Rastegar, "Two-step probabilistic method to enable demand response programs in renewable-based integrated energy systems," *CSEE Journal of Power and Energy Systems*, .